STIFFNESS, THERMAL EXPANSION, AND THERMAL BENDING FORMULATION OF STIFFENED, FIBER-REINFORCED COMPOSITE PANELS

Craig S. Collier *
Principal Structures Engineer
Lockheed Engineering and Sciences Co.
NASA Langley Research Center
Hampton, VA

ABSTRACT

A method is presented for formulating stiffness terms and thermal coefficients of stiffened, fiber-reinforced composite panels. The method is robust enough to handle panels with general cross sectional shapes, including those which are unsymmetric and/or unbalanced. Non-linear, temperature and load dependent constitutive material data of each laminate are used to "build-up" the stiffened panel membrane, bending, and membrane-bending coupling stiffness terms and thermal coefficients. New thermal coefficients are introduced to quantify panel response from through-the-thickness temperature gradients. A technique of implementing this capability with a single plane of shell finite elements using the MSC/NASTRAN™ analysis program (FEA) is revealed that provides accurate solutions of entire airframes or engines with coarsely meshed models.

An example of a composite, hat-stiffened panel is included to demonstrate errors that occur when an unsymmetric panel is symmetrically formulated as traditionally done. The erroneous results and the correct ones produced from this method are compared to analysis from discretely meshed three-dimensional FEA.

NOMENCLATURE

lamina *(i = 1, 2, 3)*

E_i	Elasticities
ν_{ij}	Poisson's ratios
α_i	Thermal expansion coefficients
Q_{ij}	Reduced stiffness terms
$\overline{Q}_{ij}$	Transformed reduced stiffness term
Φ_i	Reduced thermal stiffness terms
$\overline{\Phi}_i$	Transformed reduced thermal stiffness terms
σ_i, ϵ_i	Stresses and strains

laminate

h	Thickness
	(i = 1, 2, 3)
$\overline{Q}^*_{ij}$	Effective reduced stiffness terms
$\overline{\Phi}^*_i$	Effective reduced thermal stiffness terms

panel

H	Depth
S_x	Unit width of panel corrugation
	(i = 1, 2, 3)
M_i	Materials (particular layup) of the upper facesheet, coresheet, and bottom facesheet

laminate or panel

ΔT	In-plane temperature gradient
ΔG	Through-the-thickness temperature gradient
	(i = 1, 2, 3)
h_i	Distance from the reference plane
A_{ij}, B_{ij}, D_{ij}	Membrane, membrane-bending coupling, and bending stiffness terms
$A_i^{\alpha}, B_i^{\alpha}, D_i^{\alpha}$	Membrane, membrane-bending coupling, and bending thermal force & moment coefs.
$NA_i^{\alpha}, NB_i^{\alpha}, ND_i^{\alpha}$	MSC/NASTRAN FEA membrane, membrane-bending coupling, and bending thermal expansion & bending coefficients
	(i = x, y, xy)
α_i, α_{ci}	Thermal expansion, expansion coupling,
δ_i, δ_{ci}	bending, and bending coupling coefficients
E_i	Effective engineering elasticities
ν_{ij}	Poisson's ratios
N_i, M_i	Forces and moments
ϵ_i, κ_i	Reference plane strains and curvatures

superscripts

p	Panel
T	Thermal
M	Mechanical

---

* Senior member AIAA

INTRODUCTION

External surfaces of many of today's aircraft are designed with stiffened panels. Some various shaped stiffening members commonly used for panel structural concepts are shown in Fig. 1. The stiffening member provides the benefit of added load-carrying capability with a relatively small additional weight penalty. Though some concepts have nearly equal stiffness in both directions, most stiffened panel designs provide high bending stiffness in only one direction. Such unidirectionally designed panels are easier to manufacture and most applications do not require high bending stiffness in both directions. Thermal forces and moments induced from temperature gradients are smaller for stiffened panels than they are for sandwich type panels. These reduced thermal loads make them efficient as *hot* structure on high speed aircraft. By nature of their shapes, stiffened panels are both orthotropic and unsymmetric, even when fabricated with conventional metallic materials. (Sandwich panels become unsymmetric whenever the upper and lower facesheets have different stiffness properties, for example due to different materials.) These additional panel behaviors complicate the formulation of stiffness, thermal expansion, and thermal bending. Quantifying these behaviors is important because they significantly alter computed force, moment, curvature, strain, and stress.

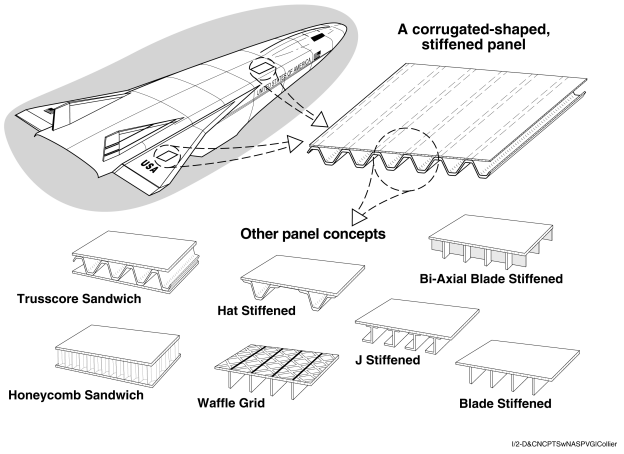

Fig. 1 The Formulation can be applied to any stiffened, composite panel concept.

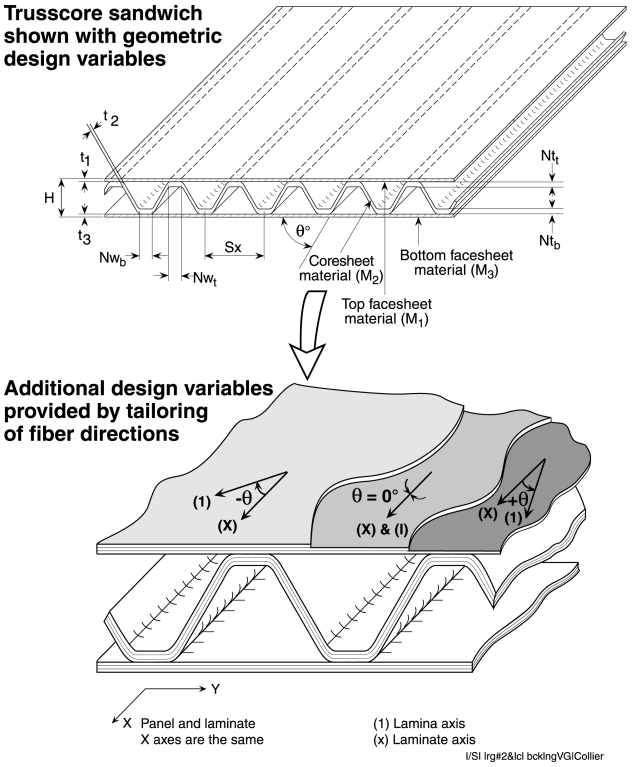

Fig. 2 The Formulation can handle the additional composite material design variables.

Treatment of Composite Materials

With the advancement of fiber-reinforced composite materials, current high speed aircraft designs use these same stiffened panel concepts incorporating the newer materials. These newer materials provide more design variables to optimize, Fig. 2**, thus improving the chances of minimizing structural weight. By taking advantage of the beneficial tailoring capability of the material, the panel facesheets and coresheet become orthotropic by themselves, further complicating stiffness, thermal expansion, and thermal bending formulations.

An expedient solution to formulating composite stiffened panel stiffness terms and thermal expansion and bending coefficients must be founded on an effective balance between the amounts of lamina and laminate data to include. An attempt to include lamina data into each stiffened panel formulation would be too complicated and hence detrimental to a design process. The challenge is to formulate panel stiffness and thermal expansion and bending behavior without knowing the particular layups or lamina material properties.

**Throughout, figures illustrate a trusscore. In this paper the trusscore is considered to be a stiffened panel because the addition of its bottom facesheet makes it a more general form of the corrugated shaped panel.

Purpose of Paper

This paper describes a formulation for stiffness terms and thermal coefficients that accurately handles these complexities. The formulations are introduced in reference 1. Their significance for a typical stiffened panel design and an entire aircraft analysis is demonstrated in references 2 and 3 respectively. This paper fully develops the formulations and validates them using discretely meshed, three-dimensional FEA.

The formulations provide a technique for effectively including lamina and laminate data in stiffened panel structural properties, while new thermal coefficients provide a means to apply through-the-thickness temperature gradients to a panel, Fig 3. Together they constitute a complete set of stiffness terms and thermal expansion and bending coefficients for stiffened, fiber-reinforced composite panels. These data are then input to the MSC/-NASTRAN^{TM} finite element analysis (FEA) program using a two-dimensional model that has a single plane of finite elements. See Fig. 4.

2-D FEA results for a typical panel design and loading are shown that demonstrate the differences between results predicted for an unsymmetric hat stiffened panel design using traditional formulation and then correctly predicted using this method's unsymmetric formulation. Finely meshed 3-D FEA is used to verify this formulation as implemented with 2-D coarsely meshed FEA.

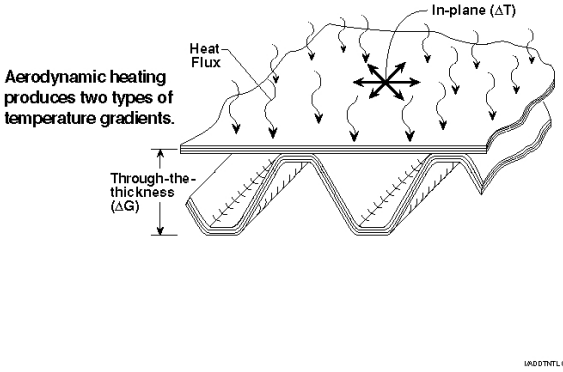

Fig. 3 Aerodynamic heating of high speed aircraft produces two kinds of temperature gradients.

Applications

These formulations are particularly useful for coarsely meshed models of a total structural entity such as an engine or airframe. Models of such large surface areas can only be accomplished with a single plane of shell finite elements. Too many elements would be necessary to construct a discrete three-dimensional model that defined the panel shapes. 3-D models are desirable because of their accuracy in capturing unsymmetric stiffness and through-the-thickness temperature gradients

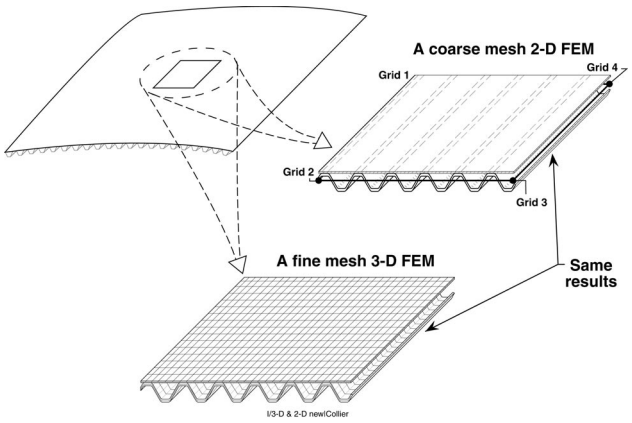

Fig. 4 Accurate results are possible with 2-D planar FEM's.

as proven with tests [4]. A planar two-dimensional model can capture these same effects by including the complete set of panel thermal and stiffness properties in a shell finite element. These planar finite element models are well suited for achieving a multidisciplined design capability for high speed aircraft.

The formulations of this paper apply to any stiffened panel concept and are intended to be coded into computer application software. They are being added to the ST-SIZE structural-thermal sizing program [3] which is linked with the MSC/NASTRAN finite element program to provide an analysis and sizing capability that can be iterated automatically until a structure's weight converges. The method could be conveniently applied to other type codes. The link to FEA is not necessary. However, due to the level of detail and mathematics involved, the techniques are not suited for hand analyses. A facility for storing and retrieving temperature and load dependent laminate data is necessary for optimization or sizing applications. The ST-SIZE program uses a material database.

Limitations and assumptions of the method fall within those usually applied in classical lamination theory [5]. A primary assumption is that strain variation through the panel cross section follows the Kirchhoff hypothesis for laminated plates. This hypothesis maintains that a normal to the midplane remains straight and normal upon panel deformation and that stresses in the XY plane govern the laminate behavior. Implications of this hypothesis are: 1) membrane strains vary linearly through the panel cross section 2) stresses vary in a discontinuous manner through the cross section 3) the facesheet laminates are perfectly bonded to the coresheets, and 4) the bonds are infinitesimally thin and non-shear deformable. This implies that ϵ^p_z, γ^p_{xz}, & $\gamma^p_{yz} = 0$, in addition to the usual *plane stress* assumption of σ^p_z, τ^p_{xz}, & $\tau^p_{yz} = 0$. For convenience, matrix terms 16, 26, & 66 are referred to as 13, 23, & 33.

STIFFNESS TERMS AND THERMAL EXPANSION & BENDING COEFFICIENTS

Panel stiffnesses and thermal coefficients are calculated by extending classical lamination theory to the stiffened cross section. Stacking sequence and lamina material properties are used to calculate orthotropic laminate properties. These laminate properties are treated as if they were individual laminae and used in extended classical lamination equations for calculating stiffened panel, orthotropic, or more general anisotropic properties. Fig. 5 illustrates the technique. Special consideration is given to the actual shape of the stiffening member and its non-plate behavior. This approach offers the capability to handle unsymmetric and unbalanced stiffened panels. The full complement of membrane, bending, and membrane - bending coupling behaviors are included in the derivation of panel stiffness terms and thermal coefficients.

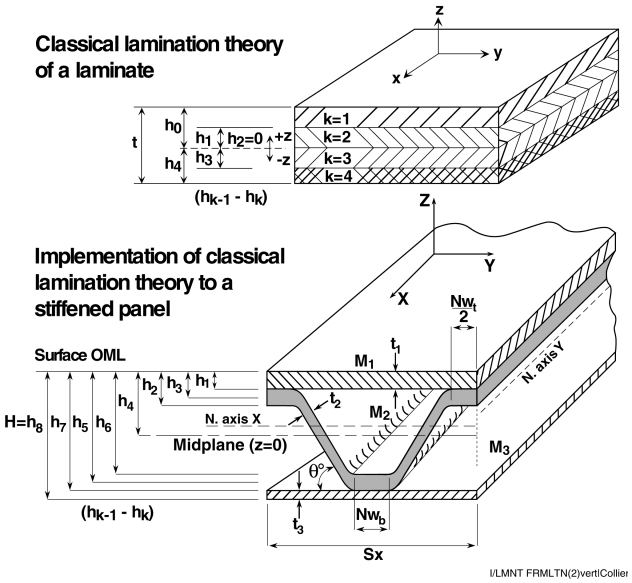

Fig. 5 Laminate formulation is extended to stiffened panels.

A stiffened panel may be formulated with each of its laminates described with membrane stiffness and membrane expansion. The benefit of this approach is that structural and thermal stiffened panel formulation can be performed efficiently by not having to work with individual ply properties of candidate laminates. Stiffness and thermal properties of candidate laminates are computed in advance and saved in a materials database. They are then divided by their thicknesses to arrive at effective stiffness and thermal terms. Thus, this panel formulation treats the facesheet and coresheet laminates as if they were laminae. A full explanation of the formulation is presented below.

Stiffness Formulation

Laminate: Laminate formulation can be summarized with the well known equations of membrane A_{ij}, membrane-bending coupling B_{ij}, and bending stiffness D_{ij},

$$A_{ij} = \sum_{k=1}^{\eta} \left(\overline{Q}_{ij}\right)_k \left(h_{k-1} - h_k\right) \qquad (1)$$

$$B_{ij} = -\frac{1}{2}\sum_{k=1}^{\eta} \left(\overline{Q}_{ij}\right)_k \left(h_{k-1}^2 - h_k^2\right)$$

$$D_{ij} = \frac{1}{3}\sum_{k=1}^{\eta} \left(\overline{Q}_{ij}\right)_k \left(h_{k-1}^3 - h_k^3\right)$$

These equations differ from others [5,6,7] because of a different sign convention. The sign convention of Fig. 5 causes the usual terms $(h^i_k - h^i_{k-1})$ to become $(h^i_{k-1} - h^i_k)$ and the B_{ij} to be negative. The rest of the laminate stiffness formulation is the same. Therefore, $\overline{Q}_{ij}$ are the transformed reduced laminae elasticities. $\overline{Q}_{ij} = Q_{ij}[T]^4$ where $[T]^4$ is a fourth order tensor and Q_{ij} are the reduced laminae elasticities. As an example

$$Q_{11} = \frac{E_x}{\left(1 - \nu_{12}\nu_{21}\right)} \qquad (2)$$

Q_{ij} are interpolated from a material database using the laminate's temperature and compression or tension stress condition.

Panel: Laminate A_{ij} from equation (1) are divided by their thicknesses to create new data entities $\overline{Q}^*_{ij}$ for use in temperature dependent and load dependent panel stiffnesses

$$A^p_{ij} = \left[\left(\overline{Q}^*_{ij}\right)_1 \left(h_0 - h_1\right) + \left(\overline{Q}^*_{ij}\right)_3 \left(h_7 - h_8\right)\right] \qquad (3)$$

$$B^p_{ij} = -\frac{1}{2}\left[\left(\overline{Q}^*_{ij}\right)_1 \left(h_0^2 - h_1^2\right) + \left(\overline{Q}^*_{ij}\right)_3 \left(h_7^2 - h_8^2\right)\right]$$

$$D^p_{ij} = \frac{1}{3}\left[\left(\overline{Q}^*_{ij}\right)_1 \left(h_0^3 - h_1^3\right) + \left(\overline{Q}^*_{ij}\right)_3 \left(h_7^3 - h_8^3\right)\right]$$

The h_i variables are illustrated in Fig. 5. They are defined as: $h_0=H/2$, $h_1=h_0-t_1$, $h_2=h_1-Nt_t$, $h_3=h_1-Nt_t/2$, $h_4=0$, $h_8=-H/2$, $h_7=h_8+t_3$, $h_6=h_7+Nt_b$, and $h_5=h_7+Nt_b/2$. Shown in Fig. 2 are the variables t_1, t_2, and t_3 which are the top facesheet, coresheet, and bottom facesheet thicknesses. Nt_t and Nt_b are the thicknesses of the coresheet top and bottom joining nodes. The subscripts 1, 2, and 3 on the $\overline{Q}^*_{ij}$ terms represent the different isotropic materials or composite layups. Properties of these materials or layups are based on their non-linear temperature and load dependent data. Equations for longitudinal stiffness terms A^p_{11}, B^p_{11}, and D^p_{11} are expanded to account for additional geometric variables such as coresheet angle θ, corrugation spacing

S_x, and widths of the coresheet top and bottom joining nodes Nw_t and Nw_b. As an example the equation for B^p_{11} is shown where the variables are shown in Fig. 5.

(Omitted in this PDF version) (4)

Even though the laminate's X axis is parallel to the panel's corrugation direction, Fig. 2, the 13 and 23 stiffness terms are non-zero when unbalanced layups are used for the facesheets. If the bottom facesheet was left off of the panel, the coresheet's contribution to the 33 terms as defined by reference 8 is likely to be relatively significant.

The terms $(\overline{Q}^*_{ij})_2 t$ and $(\overline{Q}^*_{ij})_2 b$ of equation (4) distinguish the coresheet top and bottom node laminate reduced stiffnesses from the middle coresheet reduced stiffnesses. Even though they are the same material or layup, a through-the-thickness temperature gradient causes their properties to be dissimilar.

Unlike the facesheets, the corrugated coresheet does not behave as a plate. Its nodes and mid portion strain in the longitudinal direction like a thin strip of plate or a beam. Because of this, the coresheet does not contribute to the panel stiffness terms 12, 22, 13, and 23 as omitted from equation (3). More subtle is the fact that the coresheet's contribution to panel longitudinal stiffness as included in equation (4) is not effected by plate coupling as identified by equation (2). The coresheet's accordion shape allows it to strain unconfined in the transverse direction eliminating the need for the familiar plate term $(1-\nu^2)$. Coresheet laminate membrane stiffness $(A_{11})_2$ which includes orthotropic coupling cannot be divided by its thickness to obtain $(\overline{Q}^*_{11})_2$. Instead the coresheet's uncoupled $(\overline{Q}^*_{11})_2$ terms equal the effective laminate engineering elasticity, E_x

$$E_x = \frac{A_{11}\left(1-\nu_{xy}\nu_{yx}\right)}{t} \qquad (5)$$

or more generally for unsymmetric or unbalanced laminates

$$E_x = \frac{1}{A^{-1}_{11} t} \qquad (6)$$

Thermal Coefficient Formulation

Laminate: Classical lamination thermal analysis can be summarized by equations from reference 5. First a ply's thermal stresses are computed in its fiber direction

$$\sigma^T_i = Q_{ij}\alpha_i \Delta T \qquad (7)$$

where $_i$ = the $_1$ and $_2$ ply expansion coefficients, T = the change in temperature of the ply, and subscript i refers to the ply's 1, 2, and 3 directions. Second, the ply's thermal stresses are rotated to the laminate axes using a 2nd order tensor transformation

$$\sigma^T_i = \sigma^T_i [T]^2 \qquad (8)$$

where, on the left i = x, y, & xy; and on the right i = 1, 2, & 3. Third, the ply thermal stresses are integrated with other ply thermal stresses to obtain laminate thermal forces and moments

$$\left(N^T_i, M^T_i\right) = \int_{-h/2}^{h/2} (\sigma^T_i)_k (1, -Z) dz \qquad (9)$$

where k = the ply layer and i = x, y, & xy. Equation (9) rewritten to include terms from equations (7) and (8) is

$$\left(N^T_i, M^T_i\right) = \int_{-h/2}^{h/2} (Q_{ij})_k (\alpha_i \Delta T)_k [T]^2_k (1, -Z) dz \qquad (10)$$

This formulation requires obtaining each ply's properties and orientation angle (θ) and performing the integration including the difference between each ply's initial temperature and its new elevated temperature. While integrating laminae expansion coefficients and temperature differences through the laminate depth provides thermal forces and moments, other means become necessary to compute thermal forces and moments for applications where integration cannot be performed. It is particularly convenient to be able to define thermal response of a laminate or panel independently of its current temperature condition. Described below is a new formulation unlike others [5,6,7,9,10,11] that accomplishes this in two parts. The first is defining equivaSlent plate thermal expansion, bending, and expansion-bending coupling coefficients. The second is identifying two unique gradients such that their superposition captures each ply's temperature difference.

The first and more common gradient is referred to informally as in-plane (ΔT) which designates the laminates change in temperature at a reference plane. (Strictly speaking, an in-plane gradient quantifies the temperature change on a surface. This data is captured by the FEM mesh.) The second gradient called through-the-thickness (ΔG), defines a linear variation of temperature through a

laminate's depth. Therefore a ply's $\Delta T = f(\Delta T, Z\ G)$ of the laminate's depth. Therefore a ply's $\Delta T = f(\Delta T, Z\Delta G)$ of the laminate. By defining the terms $\Phi_i = Q_{ij}\alpha_i$ and $\overline{\Phi}_i = \Phi_l[T]^2$, equation (10) can be written as

$$\left(N_i^T, M_i^T\right) = \int_{-h/2}^{h/2} (\overline{\Phi}_i)_k (\Delta T + Z\Delta G)(1, -Z)dz \tag{11}$$

which, by performing the integration and writing in matrix notation becomes

$$\begin{Bmatrix} N_i^T \\ M_i^T \end{Bmatrix} = \begin{bmatrix} \sum_{k=1}^{\eta} \left(\overline{\Phi}_i\right)_k \left(h_{k-1} - h_k\right) & -\frac{1}{2}\sum_{k=1}^{\eta} \left(\overline{\Phi}_i\right)_k \left(h_{k-1}^2 - h_k^2\right) \\ -\frac{1}{2}\sum_{k=1}^{\eta} \left(\overline{\Phi}_i\right)_k \left(h_{k-1}^2 - h_k^2\right) & \frac{1}{3}\sum_{k=1}^{\eta} \left(\overline{\Phi}_i\right)_k \left(h_{k-1}^3 - h_k^3\right) \end{bmatrix} \begin{bmatrix} \Delta T \\ -\Delta G \end{bmatrix} \tag{12}$$

Equation (12) is abbreviated to

$$\begin{Bmatrix} N_i^T \\ M_i^T \end{Bmatrix} = \begin{bmatrix} A_i^\alpha & B_i^\alpha \\ B_i^\alpha & D_i^\alpha \end{bmatrix} \begin{bmatrix} \Delta T \\ -\Delta G \end{bmatrix} \tag{13}$$

by identifying thermal force A_i^α, moment D_i^α, and force-moment coupling B_i^α coefficients

$$\begin{aligned} A_i^\alpha &= \sum_{k=1}^{\eta} \left(\overline{\Phi}_i\right)_k \left(h_{k-1} - h_k\right) \\ B_i^\alpha &= -\frac{1}{2}\sum_{k=1}^{\eta} \left(\overline{\Phi}_i\right)_k \left(h_{k-1}^2 - h_k^2\right) \\ D_i^\alpha &= \frac{1}{3}\sum_{k=1}^{\eta} \left(\overline{\Phi}_i\right)_k \left(h_{k-1}^3 - h_k^3\right) \end{aligned} \tag{14}$$

Note the similarity of these to the formulation of the A_{ij}, D_{ij}, and B_{ij} stiffness terms of equation (1). Other than the substitution of $\overline{Q}_{ij}$ with $\overline{\Phi}_i$, the only other difference between the equations is the treatment of X & Y orthotropic coupling. Stiffness formulation defines separate terms to account for directional coupling. Thermal formulation defines orthotropic coupling at the lamina level as shown in equation (7), reference 5, and with the Φ_i term of this method. Doing this reduces what would have been 3x3 matrix coefficients into 3x1 vector coefficients.

Thermal forces and moments are added to mechanical forces and moments to produce the system equations

$$\begin{Bmatrix} N_i \\ M_i \end{Bmatrix} = \begin{Bmatrix} N_i^M \\ M_i^M \end{Bmatrix} + \begin{Bmatrix} N_i^T \\ M_i^T \end{Bmatrix} = \begin{bmatrix} A_{ij} & B_{ij} \\ B_{ij} & D_{ij} \end{bmatrix} \begin{Bmatrix} \varepsilon_i^M + \varepsilon_i^T \\ \kappa_i^M + \kappa_i^T \end{Bmatrix} \tag{15}$$

These combined thermomechanical forces and moments follow the same rules and are used the same as mechanical only loading. Consequently, thermal loads multiplied by the combined 6x6 inverted stiffness matrix provides thermal strains and curvatures

$$\begin{Bmatrix} \varepsilon_i^T \\ \kappa_i^T \end{Bmatrix} = \begin{bmatrix} A_{ij} & B_{ij} \\ B_{ij} & D_{ij} \end{bmatrix}^{-1} \begin{Bmatrix} N_i^T \\ M_i^T \end{Bmatrix} \tag{16}$$

By adding equation (13) to equation (16), thermal growth can be rewritten as

$$\begin{Bmatrix} \varepsilon_i^T \\ \kappa_i^T \end{Bmatrix} = \begin{bmatrix} A_{ij} & B_{ij} \\ B_{ij} & D_{ij} \end{bmatrix}^{-1} \begin{Bmatrix} A_i^\alpha \Delta T - B_i^\alpha \Delta G \\ B_i^\alpha \Delta T - D_i^\alpha \Delta G \end{Bmatrix} \tag{17}$$

By setting $\Delta G = 0$, two in-plane gradient, thermal expansion coefficients are identified

$$\begin{Bmatrix} \alpha_i \\ \alpha_{ci} \end{Bmatrix} = \begin{bmatrix} A_{ij} & B_{ij} \\ B_{ij} & D_{ij} \end{bmatrix}^{-1} \begin{Bmatrix} A_i^\alpha \\ B_i^\alpha \end{Bmatrix} \tag{18}$$

By setting $\Delta T = 0$, two through-the-thickness gradient, thermal bending coefficients are introduced

$$\begin{Bmatrix} \delta_{ci} \\ \delta_i \end{Bmatrix} = \begin{bmatrix} A_{ij} & B_{ij} \\ B_{ij} & D_{ij} \end{bmatrix}^{-1} \begin{Bmatrix} B_i^\alpha \\ D_i^\alpha \end{Bmatrix} \tag{19}$$

The subscript c indicates expansion-bending coupling. These coupling coefficients delineate the unsymmetric response due to ΔT and ΔG temperature gradients. α_i and δ_{ci} quantify thermal strain for a ΔT and ΔG respectively, and α_{ci} and δ_i quantify thermal curvature for a ΔG and ΔT respectively.

$$\begin{Bmatrix} \varepsilon_i^T \\ \kappa_i^T \end{Bmatrix} = \begin{Bmatrix} \alpha_i \\ \alpha_{ci} \end{Bmatrix} \Delta T - \begin{Bmatrix} \delta_{ci} \\ \delta_i \end{Bmatrix} \Delta G \tag{20}$$

All 12 of these unique thermal coefficients and both of the in-plane and through-the-thickness temperature gradients contribute to thermal forces and to thermal moments. Together they explicitly quantify unsymmetric and unbalanced response caused by unsymmetric and unbalanced stiffness and by unsymmetric and unbalanced thermal expansion and bending.

$$\begin{Bmatrix} N_i^T \\ M_i^T \end{Bmatrix} = \begin{bmatrix} A_{ij} & B_{ij} \\ B_{ij} & D_{ij} \end{bmatrix} \begin{Bmatrix} \alpha_i \Delta T - \delta_{ci} \Delta G \\ \alpha_{ci} \Delta T - \delta_i \Delta G \end{Bmatrix} \tag{21}$$

In contrast to the familiar equation (10), equations (13), (20), and (21) are able to quantify thermal response independently of current laminate temperature profile. This is accomplished by taking the ply's T and α_1 and α_2

out of the integration and supplying instead laminate expansion, bending, and expansion-bending coupling coefficients and in-plane and through-the-thickness temperature gradients. In essence, these thermal coefficients are smeared equivalent plate values which are based on a through the depth integration. These smeared equivalent plate stiffnesses and thermal coefficients can then be accurately used for FEA.

Panel: Panel implementation of thermal lamination theory follows the approach of panel stiffness formulation. As a consequence, non-linear, temperature and load dependent laminate force coefficients, A_i^{α}, are divided by laminate thickness to give $\overline{\Phi}_i^{\,*}$ for use in developing panel force and moment thermal coefficients. Note how their formulation follows panel stiffness formulation.

$$\begin{aligned} A_i^{p\alpha} &= \left[\left(\overline{\Phi}_i^{*}\right)_1\left(h_0-h_1\right)+\left(\overline{\Phi}_i^{*}\right)_3\left(h_7-h_8\right)\right] \\ B_i^{p\alpha} &= -\frac{1}{2}\left[\left(\overline{\Phi}_i^{*}\right)_1\left(h_0^2-h_1^2\right)+\left(\overline{\Phi}_i^{*}\right)_3\left(h_7^2-h_8^2\right)\right] \\ D_i^{p\alpha} &= \frac{1}{3}\left[\left(\overline{\Phi}_i^{*}\right)_1\left(h_0^3-h_1^3\right)+\left(\overline{\Phi}_i^{*}\right)_3\left(h_7^3-h_8^3\right)\right] \end{aligned} \qquad (22)$$

Equations for the longitudinal coefficients $A_1^{p\alpha}$, $B_1^{p\alpha}$, and $D_1^{p\alpha}$ are expanded to account for the corrugated shape as exemplified with equation (4). The complete set of panel thermal force and moment coefficients are then used to define temperature dependent panel expansion, α^p & α_c^p, and bending, δ^p & δ_c^p, coefficients following equations (18) and (19).

The coresheet's corrugated shape allows it to expand freely in the transverse direction precluding it from contributing to the panel transverse or shear thermal force and moment coefficients: $A_2^{p\alpha}$, $A_3^{p\alpha}$, $B_2^{p\alpha}$, $B_3^{p\alpha}$, $D_2^{p\alpha}$, and $D_3^{p\alpha}$. More subtle however, is the way the corrugated coresheet contributes to the longitudinal force and moment coefficients, $A_1^{p\alpha}$, $B_1^{p\alpha}$, and $D_1^{p\alpha}$. Since its nodes and mid section expand almost entirely unrestrained in the transverse direction as separate strips of plates or beams, its thermal formulation must not contain the embedded X and Y directional coupling that is innate to classical lamination thermal formulation. This need for a non-plate thermal formulation is consistent with the need for a non-plate stiffness formulation as described for equations (5) and (6). The solution for uncoupling the longitudinal stiffness from the transverse stiffness was to omit the familiar Poisson's plate term $(1-\nu^2)$ from the coresheet formulation. Uncoupling of a coresheet's laminate longitudinal thermal behavior from its transverse behavior can be accomplished two ways. First the behavior of stacked lamina can be computed omitting lamina properties that contribute to the laminate Y axis (transverse direction). Unfortunately this requires additional layup computations and saving more data in a material database. Another way to arrive at a laminate's uncoupled $\overline{\Phi}_i^{\,*}$ is by

$$\overline{\Phi}_1^{\,*} = \alpha_x E_x \qquad (23)$$

where α_x is from equation (18) and E_x is from equation (6).

APPLICATION WITH FEA

In-plane and through-the-thickness temperature gradients can be correctly applied and solved for anisotropic/orthotropic, unsymmetric, and unbalanced laminates or stiffened panels with a single plane of shell elements with the MSC/NASTRAN FEA program. This is accomplished by including the full complement of smeared equivalent plate stiffness matrices and thermal expansion and bending coefficient vectors in the FEM data deck. Stiffness matrices for membrane, bending, and membrane-bending coupling are entered directly into MSC/NASTRAN with only minor adjustments [12]. Thermal expansion and bending coefficient vectors for membrane, bending, and membrane-bending coupling cannot be entered into MSC/NASTRAN without major adjustments to their formulation [1].

MSC/NASTRAN Thermal Coefficients

A technique is introduced to identify nine unique MSC/-NASTRAN thermal coefficients, NA_i^{α}, NB_i^{α}, and ND_i^{α} in order to compute thermal loads. MSC/NASTRAN computes thermal forces and moments by

$$\begin{aligned} N_i^T &= A_{ij}NA_i^{\alpha}\Delta T - B_{ij}NB_i^{\alpha}\Delta T \\ M_i^T &= B_{ij}NB_i^{\alpha}\Delta T - D_{ij}ND_i^{\alpha}\Delta G \end{aligned} \qquad (24)$$

Where the stiffness matrices and thermal coefficient vectors shown can represent either a laminate or a stiffened panel. MSC/NASTRAN uses the same sign convention as the formulation of this paper. Their coefficients can be found by equating equation (24) to equation (13) and solving for ΔT and ΔG separately

$$\begin{aligned} NA_i^{\alpha} &= A_{ij}^{-1}A_i^{\alpha} \\ NB_i^{\alpha} &= B_{ij}^{-1}B_i^{\alpha} \\ ND_i^{\alpha} &= D_{ij}^{-1}D_i^{\alpha} \end{aligned} \qquad (25)$$

Because equation (24) does not join thermal force calculation with moment calculation, the ensuing stiffness matrices of equation (25) are inverted separately. These inverted 3x3 matrices are unlike the 6x6 inverted stiffness matrix of the other equations.

Temperature and load dependent stiffnesses and thermal coefficients are placed on the MSC/NASTRAN MAT2 data record. A change in the panel's bulk temperature is entered in the FEA by supplying the reference temperature on the MAT2 record and the loadcase dependent temperature on the TEMPP1 record. The effect of in-plane temperature gradients is then captured with the model's discretization. Loadcase dependent through-the-thickness gradients are entered on an element basis with the TEMPP1 record.

Model Reference Plane

FEM grid points are customarily located at a panel's midplane as depicted in the 2-D FEM of Fig. 4. Typically a structural analyst will choose the aerodynamically defined outer mold line (OML) as his FEM's surface. This causes the midplane of the structural surface to be in error; however, this is ordinarily done due to the difficulty of offsetting CAD generated lofted surfaces. This error causes an unconservative calculation of a structure's bending stiffness. While perhaps not significant for an airframe fuselage, this inaccuracy is substantial for wings and other shallow structural components. Another short-coming of this approach, as displayed in Fig. 6, is that even though an analyst might go through the effort of offsetting his model properly, his offset is usually based on an assumed panel depth that is likely to change as strength and stability analyses are performed.

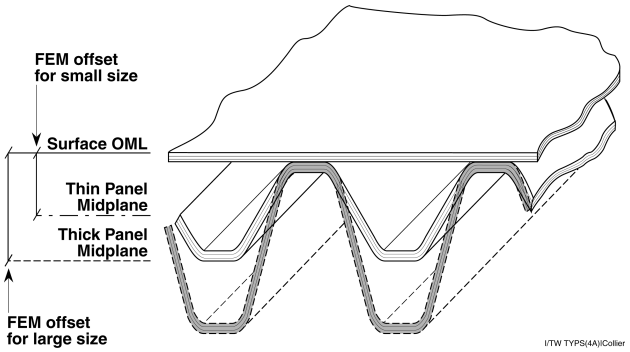

Fig. 6 The best choice of a FEM reference plane is the surface outer mold line.

A solution to these shortcomings is to always use the OML for the location of FEM grid points. This can be accurately achieved by redefining the panel's reference plane from the midplane as established in Fig. 5 to the OML as illustrated in Fig. 7. By using the OML as the panel's reference plane, the h_i variables are calculated as: $h_0=0$, $h_1=-t_1$, $h_2=h_1-Nt_t$, $h_3=h_1-Nt_t/2$, $h_4=-H/2$, $h_8=-H$, $h_7=h_8+t_3$, $h_6=h_7+Nt_b$, and $h_5=h_7+Nt_b/2$. All of the previously defined equations of stiffness and thermal coefficients can still be used exactly as formulated. Higher panel bending stiffnesses will be calculated this way but they will be balanced out with higher membrane-bending coupling stiffnesses. Note that a symmetric panel will now have non-zero membrane-bending coupling data.

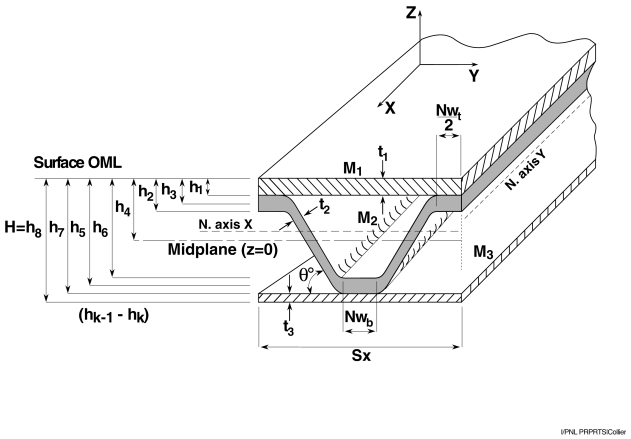

Fig. 7 The surface outer mold line can be conveniently used as the FEM reference plane.

Regardless of choice of reference plane, the resulting FEA thermomechanical forces and moments are used to compute panel strains and curvatures as defined with equation (15). Strains at any location can easily be established since strains are formulated to vary linearly through panel depth. A laminate strain is the summation of the panel's reference plane strain and the additive or subtractive contribution of the curvature

$$\{\varepsilon_i\}_m = \varepsilon_i^p - \kappa_i^p H_m \qquad (26)$$

where H_m is the distance between the reference plane and the panel depth location m.

LOAD DEPENDENT RESIDUAL STRAINS

Residual panel strains and stresses caused by thermal growth are resolved on a laminate basis for each loadcase. They develop in stiffened panels when the panel laminates want to elongate non-uniformly when heated. Because the panel laminates cannot act independently, they develop residual strains and stresses when forced to strain together as a unit of the panel. Panel curvature dictates that all laminate strains follow its through-the-depth strain profile. This profile is linear due to Kirchoff's hypothesis that a normal to the midplane remains straight and normal upon panel deformation. The residual strain is the difference between the strain that occurs in the laminate when made a segment of the stiffened panel's linear strain profile, and the strain that occurs in the laminate when allowed to thermally grow unattached to the panel.

2-D FEA is able to use smeared equivalent plate properties for a stiffened panel because of this "plane sections remain plane" hypothesis. In principle, during FEA, panel laminates strain together as a unit providing a linear strain profile through-the-depth, and thus do not include residuals. In order to quantify a laminate's "design-to" strains, its residual strains must also be quantified and added to FEA computed strains. Fig. 8 summarizes this process.

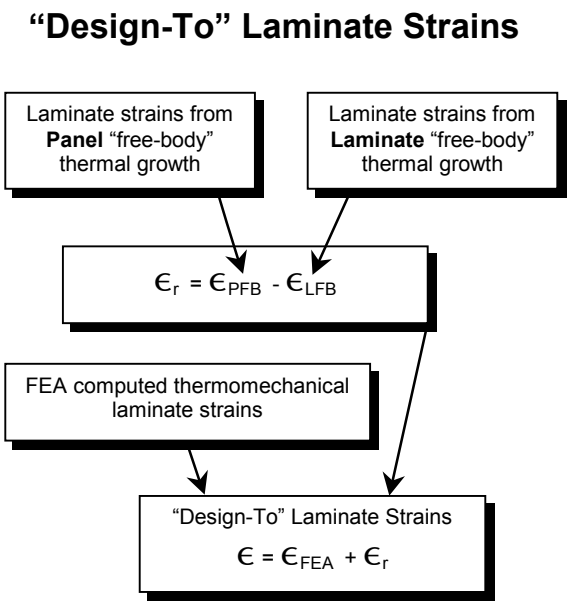

Fig. 8 Three types of computed strain contribute to laminate "design-to" strains.

Laminate strains from **laminate** "free-body" thermal growth, (left top box of Fig. 8) are computed with either equation (16), (17) or (20). In this case ΔT is the laminate's change in temperature which includes both panel ΔT and ΔG. Laminate strains from **panel** "free-body" thermal growth are computed first by using, again, equation (16), (17), or (20) (this time with panel data instead of laminate data) and second, by using these panel strains and curvatures with equation (26) to obtain laminate strains. Finally, FEA computed forces and moments that solve the internal load redistribution of the indeterminate structure are used in conjunction with equations (15) and (26) to arrive at thermomechanical laminate strains. All three of these computed thermal strains are required to determine "design-to" laminate strains.

TYPICAL STIFFENED PANEL ANALYSIS

The fuselage and wing skins of high speed vehicles are commonly designed with stiffened panels. A hat stiffened, fiber-reinforced, metal matrix composite is used for this example, Fig. 9. Metal matrix composites are chosen for their high temperature capability, some having a service use up to 1300°F. When allowing a stiffened panel to reach these high temperatures, its large membrane, bending, and membrane-bending coupling thermal response must be analytically quantified.

Panel Design and Temperatures

The panel cross section shape, dimensions, and laminate layups are those which are commonly produced by structural sizing optimization codes. The hat shape is fabricated by brazing the facesheet to the corrugated coresheet. Shown to the left of the section is the temperature profile which is typical of those analyzed for high speed flight. The panel's midplane temperature is 625 F. while its hottest point is on top of the facesheet (850 F.) and its coldest point is on the bottom of the coresheet (400 F.). These laminate temperatures are well within the material's limit. The shaded rectangle represents a uniform in-plane gradient of 555 F (625 F-70 F). The double shaded triangles represent a through-the-thickness gradient of 300 F/in. By superimposing the two gradients, the variation of temperature through the panel's depth is known, as illustrated with the bold line. The facesheet's average temperature of 842.5 F. and the coresheet's average temperatures of 832.75 F., 617.5 F., and 402.25 F. are used for interpolating the material database. Laminate material properties are also retrieved from the database according to compression or tension stress conditions. Compression elasticities of metal matrix composites are approximately 35% higher than their tension elasticities at elevated temperatures. These load and temperature dependent laminate data $\overline{Q}^*_{ij}$ and $\overline{\Phi}^*_i$ are used for formulating panel stiffness terms and thermal coefficients as defined with equations (3), (4), and (22).

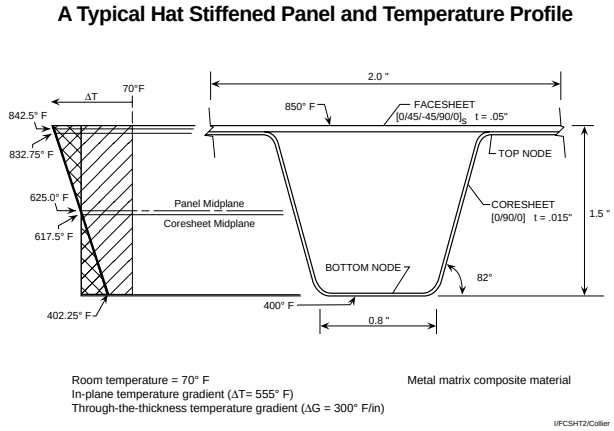

Fig. 9 Typical hat stiffened panel and temperature profile.

Panel Data

The typical corrugated stiffened panel has the following properties when this general anisotropic formulation is used. The equivalent orthotropic plate data shows the "13" and "23" terms of the stiffness matrices and the "3" terms of the thermal coefficient vectors to be zero because the laminates are balanced. If the laminates were not balanced,

$$A^p_{ij} = \begin{bmatrix} 1400599 & 259740 & 0.0 \\ 259740 & 697134 & 0.0 \\ 0.0 & 0.0 & 201010 \end{bmatrix}$$

$$B^p_{ij} = \begin{bmatrix} -549085 & -188311 & 0.0 \\ -188311 & -505422 & 0.0 \\ 0.0 & 0.0 & -145732 \end{bmatrix}$$

$$D^p_{ij} = \begin{bmatrix} 595340 & 136580 & 0.0 \\ 136580 & 366577 & 0.0 \\ 0.0 & 0.0 & 105698 \end{bmatrix}$$

The hat panel stiffness terms.

$$\alpha_i^p = \begin{Bmatrix} 3.7562 \\ 4.5833 \\ 0.0 \end{Bmatrix} 10^{-6} \qquad \alpha_{ci}^p = \begin{Bmatrix} -0.2700 \\ 0.1006 \\ 0.0 \end{Bmatrix} 10^{-6}$$

$$\delta_i^p = \begin{Bmatrix} 3.8055 \\ 4.5649 \\ 0.0 \end{Bmatrix} 10^{-6} \qquad \delta_{ci}^p = \begin{Bmatrix} -0.0946 \\ 0.0353 \\ 0.0 \end{Bmatrix} 10^{-6}$$

The hat panel thermal expansion and bending coefficients.

$$A_i^{p\alpha} = \begin{Bmatrix} 6.5807 \\ 4.1708 \\ 0.0 \end{Bmatrix} 10^{-6} \quad B_i^{p\alpha} = \begin{Bmatrix} -3.0726 \\ -3.0238 \\ 0.0 \end{Bmatrix} 10^{-6}$$

$$D_i^{p\alpha} = \begin{Bmatrix} 2.9344 \\ 2.1931 \\ 0.0 \end{Bmatrix} 10^{-6}$$

The hat panel thermal force and moment coefficients.

or if an off axis reference direction was used for the panel, these terms would not be zero and fully populated, equivalent plate, anisotropic data would have been produced. The midplane was used as the reference plane in lieu of the OML for ease of comparison to traditional methods which use neutral axes as reference planes. Note that the absolute values of the membrane-bending coupling B_{ij} terms are as large as the bending D_{ij} terms and that all of the thermal coefficients are different values which indicates the significance of the unsymmetric nature of the panel. The highest thermal coefficient is 4.6^{-6} (in-F /in), less than values of typical metallic materials. Consequently, the behavior of this panel with isotropic, metallic materials would be similar, yet amplified.

Panel Results

Thermal forces, moments, strains, and curvatures were computed to compare results of different analysis methods. It was desired to ground the various analytical results to test data. However the author was unable to obtain applicable test data for a stiffened, metal matrix composite panel that had a through-the-thickness temperature gradient applied to it or some other in-service type temperature distribution. In lieu of test data, the best possible structural-thermal analysis was performed to arrive at baseline results. Baseline strains, curvatures, forces, and moments were acquired by rigorous analysis of each of the panel's laminates which included executing classical lamination codes. Each laminate's thermal response was used to assemble the panel's response maintaining the equilibrium of forces and moments and the simultaneous compatibility of the six strain and curvature degrees of freedom of the panel.

3-D FEA of the panel was performed to provide a check of the baseline results. A finely meshed model consisting of 2400 MSC/NASTRAN CQUAD4 shell elements, similar to the 3-D FEM portrayed in figure 4, was built and executed. Since elements were included to model the coresheet corrugation pattern, the unsymmetric nature of the panel was captured. Each element used temperature dependent laminate stiffnesses [A] & [D] and thermal coefficients $\{A^\alpha\}$ & $\{D^\alpha\}$ generated by classical lamination codes. This data was input without modification directly into the MAT2 material data cards.

Two different types of 2-D FEA were performed for the panel. The first type used this formulation and is later referred to as the unsymmetric 2-D FEA. The other analysis uses traditional stiffened panel formulation and is referred to as the symmetric 2-D FEA because it ignores unsymmetric behavior. The only difference between these models is the stiffness and thermal coefficient input data. All other model data is identical. These models are different from the 3-D FEM in that they have smeared equivalent plate properties and do not have elements that model the coresheet corrugation. However the mesh density (800 elements) and connectivity of the facesheet surface is the same.

Two different panel boundary conditions are analyzed. The first condition prevents the panel from straining or curving upon applied temperature loads. This condition may be visualized as restraining the panel's growth within rigid walls. Consequently the full magnitude of induced thermal forces and moments develop, Table 1. The second boundary condition allows full thermal growth by constraining the panel in the FEM only at the center grid to prevent rigid body motion. Thermal forces and moments are zero for this case, Fig. 10, 11. These two boundary condition cases are the extremes of in-service possibilities and therefore band the level of accuracy expected for actual conditions. Analysis of the orthotropic panel with these boundary conditions cause γ^p_{xy}, κ^p_{xy}, N_{xy}, and M_{xy} to be zero, and to not be part of the solution. If the panel happened to be anisotropic, or be constrained in a way to develop shear loads, these responses would come into play.

Table 1 Comparison of computed panel forces and moments to the temperature gradients.

	Baseline results	2-D FEA Unsymm.	3-D FEA	2-D FEA Symm.
N_x	-4574	-4574	-4595	-3652
N_y	-3222	-3222	-3223	-2315
M_x	2586	2586	2581	1891
M_y	2336	2336	2337	1678

The exact match between 2-D unsymmetric FEA computed forces and moments and the baseline results is not surprising. This happens because the constrained boundary conditions (rigid walls) do not allow the element shape functions to come into play. The agreement is actually a substantiation of the defined MSC/NASTRAN force and moment equations (24) and thermal coefficients

(25). The second boundary condition where growth is permitted is more of a measure of the 2-D FEM's ability to capture the panel's unsymmetric behavior. In some respects, the good agreement to the 3-D FEM's double curvature deformed shape, Fig. 10, gives credence to the Kirchoff hypothesis of plane sections remain plane and linear strain distribution through plate thickness (in this case panel depth) as implemented with the smeared equivalent plate approach. The agreement also confirms the application of this formulation to unsymmetric stiffened composite panels and the facility to capture both the in-plane and through-the-thickness temperature gradients with the newly defined expansion, bending, and expansion-bending coupling thermal coefficients. Because symmetric 2-D FEA omits this additional data, its deformed shape caused by the uniform temperature increase exhibits zero curvature.

Symmetric 2-D FEA of traditional methods significantly under predicts both mechanical and thermal panel response. This is due to dissimilarities in the formulations of panel stiffness terms and thermal coefficients. Traditional formulations currently being practiced [13,14] require treating each layup type with different approximations, calculating neutral axes, effective thicknesses, effective areas (EA), effective moment-of-inertias (EI), effective elasticities, etc. in both the X and Y directions separately using modular ratios and the parallel axis theorem; thus treating the panel as two detached perpendicular beams. Doing this omits panel strain compatibility because the X-face unit width section is not coupled with the Y-face unit width section. Attempts to couple the directions would be in error since the X-face neutral axis does not lay on the Y-face neutral axis. Finally, membrane-bending coupling of unsymmetric stiffness, $[B^p]$, and the membrane-bending coupling of unsymmetric thermal expansion and bending, $\{\alpha_c^p\}$, $\{\delta^p\}$, $\{\delta_c^p\}$, and $\{B^{p\alpha}\}$ are missing.

In order to get the most accurate solution with the 2-D symmetric FEA, the FEM input data included X & Y plate coupling as produced by the 3x3 membrane and bending stiffness matrices and in the six expansion and bending thermal coefficients. The 2-D symmetric FEM also contained the through-the-thickness gradient. This FEA, although, was not able to include load dependent residual strains.

Panel laminate strains graphed in Fig. 11 were analyzed for strength and stability. The incorrect 2-D symmetric margin-of-safety is +0.23 indicating the panel is slightly oversized. Correct unsymmetric analysis produces a -0.06 margin, signifying panel failure.

The reported moments of Table 1 are those values found at the panel midplane. Unlike forces, the magnitude of moments vary according to the location of their reference planes. Traditional symmetric analysis uses the neutral axes for reporting moment. Accordingly, at the X-face neutral axis $M_x = 792$ and at the Y-face neutral axis $M_y = 0.0$. However, moments have limited usefulness at the neutral axes because they cannot be coupled.

The unsymmetric 2-D FEA actually compares better to the baseline results than the 3-D FEA. This could be caused by an innate shortcoming of the 3-D FEM which is due to the top joining node of the coresheet and the facesheet being modeled as if they lay on the same plane. The actual

Fig. 10 FEA deformed plots of the panel response to a uniform temperature increase of 555 F.

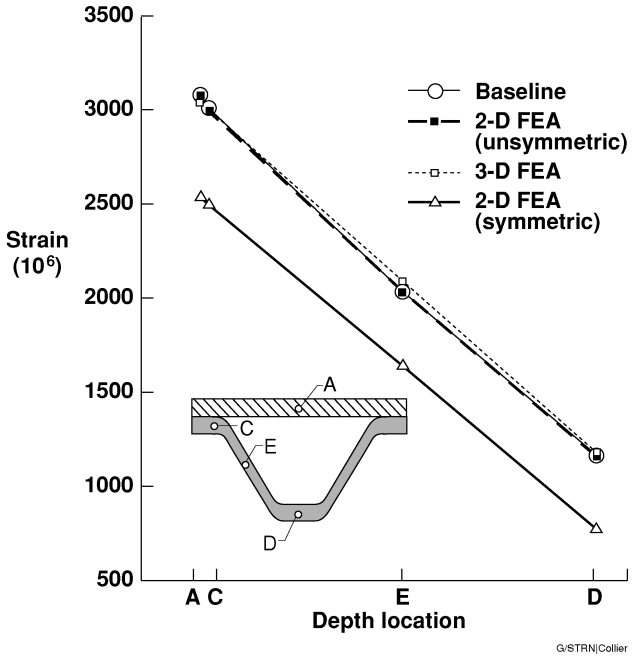

Fig. 11 Comparison of computed panel "design-to" strains (with residuals) to the temperature gradients.

separation between them is equal to $t_l/2 + Nt_t/2$, see Fig. 2. This distance is not contained in the 3-D FEM because the same grid points are needed for connecting the coresheet elements to the facesheet elements. After making minor adjustments to account for the top of the coresheet being modeled on the same plane as the facesheet, the 3-D FEM produces nearly the same results as the baseline. However, the 36" square hat panel requires at least 560 elements in order to capture the corrugated shape of the coresheet, (one element is needed to span the panel depth). With 560 elements, thermal M_x has a -2.8% error. By using an equivalent plate 2-D FEM, only one element is needed for the 36" panel while still maintaining 0% error.

CONCLUSIONS

Formulations presented in this paper provide the capability to represent a stiffened composite panel of any

geometrical cross sectional shape as an equivalent anisotropic plate. The formulations are able to accept any applied thermomechanical load combination and quantify load dependent residual thermal strains. This capability is founded on the Kirchoff hypothesis of linear strain distribution through a plate's thickness. The benefit of the hypothesis is provided by:

* extending classical lamination theory to the formulation of stiffened panels

* defining explicit thermal coefficients of membrane, bending, and membrane-bending coupling for both in-plane and through-the-thickness temperature gradients

* including temperature dependent, load dependent, non-linear material data in the constitutive formulation of each laminate's stiffness terms and thermal coefficients that build-up the stiffened panel properties

A major benefit of formulating stiffened panels with smeared equivalent plate properties is that a coarsely meshed 2-D FEM with a single plane of shell finite elements can be used to accurately analyze complex thermomechanically loaded structures. Traditional methods of formulating equivalent plate panel stiffness and thermal coefficients, though intuitive, are difficult to use for a wide possibility of applications. More importantly they give incorrect results as demonstrated. 2-D FEA that uses this formulation correlates very well with 3-D FEA.

ACKNOWLEDGEMENTS

This work was performed for the Systems Analysis Office/National Aero-Space Plane Office under NASA contract NAS1-19000 at Langley Research Center in Hampton, Virginia.

REFERENCES

[1] Collier, C.S., *COMPOSITE STIFFENED PANELS: Part 1 - Stiffness, Thermal Expansion, and Thermal Bending Formulation for Finite Element Analysis*, NASP CR 1134, April 1992

[2] Collier, C.S., "A General Method for Structural Analysis and Sizing of Composite Stiffened Panels Using 2-D Finite Element Models", NASP Technology Review, Monterey, CA, April 21-24, 1992, Paper No. 212

[3] Collier, C.S., "Structural Analysis and Sizing of Stiffened, Metal Matrix Composite Panels for Hypersonic Vehicles", AIAA 4th International Aerospace Planes Conference, Orlando, FL, December 1-4, 1992, Paper No. AIAA-92-5015

[4] Percy,W.C. and Fields,R.A., "Buckling of Hot Structures", 8th NASP Symposium, Monterey, CA, March 26-30, 1990

[5] Jones,R.M., *Mechanics of Composite Materials*, Hemisphere Publishing Corporation, Washington, DC, 1975

[6] Halpin,J.C., *Primer on Composite Materials: Analysis*, Technomic Publishing Company, Inc., Lancaster, PA, 1984

[7] Tsai,S.W., *Mechanics of Composite Materials, Part II -Theoretical Aspects,* Technical Report AFML-TR-66-149, Part II, Nov. 1966

[8] Stroud,J.W. and Arganoff,N., *Minimum-Mass Design of Filamentary Composite Panels Under Combined Loads: Design Procedure Based on Simplified Buckling Equations*, NASA TN D-8257, Oct. 1976

[9] Hahn,H.T. and Pagano,N.J., "Curing Stresses in Composite Laminates", *J. Composite Materials*, Vol.9, 1975 ,p.91

[10] Dennis,S.T., *Unsymmetric Laminated Gr/Ep Composite Plate and Beam Analysis for Determining Coefficients of Thermal Expansion*, M.S. Thesis MIT, Feb. 1983.

[11] Ishikawa,T. and Chou,T.W., "In-plane Thermal Expansion and Thermal Bending Coefficients of Fabric Composites," Proceedings of the ASME Winter Annual Meeting, Nov. 14-19, 1982, p.115-120

[12] The MacNeal-Schwendler Corporation, *MSC/-NASTRAN User's Manual*, Vol 1, Version 67, The MacNeal-Schwendler Corporation, Los Angeles, CA, Aug. 1991

[13] *Advanced Composites Design Handbook,* The Boeing Company, Seattle, WA, Sept., 1985

14 Haftka,R.T., Gurdal,Z., and Kamat,M.P., *Elements of Structural Optimization*, Kluwer Academic Publishers, The Netherlands, 1990

TRADEMARKS